Asymmetric Autocatalysis

DOI: 10.1002/anie.201304284

Asymmetric Autocatalysis Induced by Cinnabar: Observation of the Enantioselective Adsorption of a 5-Pyrimidyl Alkanol on the Crystal Surface**

Hitoshi Shindo, Yusuke Shirota, Kaori Niki, Tsuneomi Kawasaki, Kenta Suzuki, Yuko Araki, Arimasa Matsumoto, and Kenso Soai**

The origin of biological homochirality, leading to overwhelming enantioenrichment, such as that seen in L-amino acids and D-sugars, is a significant topic of interest.[1] Chiral surfaces[2] of natural minerals have been considered as a possible source of chirality.[3] Although the potential for differential adsorption of organic compounds on chiral surfaces has been mentioned,[3c] apparent chiral selection has rarely been reported.[4]

Previously, we found asymmetric autocatalysis by a 5-pyrimidyl alkanol in the addition reaction of diisopropylzinc (iPr$_2$Zn) to pyrimidine-5-carbaldehyde.[5–8] In this reaction, chiral inorganic crystals such as quartz[9a] and $NaClO_3$[9b] can act as the origin of chirality[10] to afford a highly enantioenriched product in combination with asymmetric autocatalytic amplification of enantiomeric excess.

Naturally occurring cinnabar, mercury(II) sulfide (α-HgS), is a known chiral mineral (Figure 1a,b).[11] Enantiomorphous (*P*)- and (*M*)-crystals of cinnabar[12,13] belong to the chiral space groups $P3_121$ and $P3_221$, respectively, and is constructed with -S-Hg-S-Hg- spiral chains. The screw axes are parallel to the *c* axis of the hexagonal crystal. Cinnabar has been used as a red pigment for official seal stamps in Japan and China for centuries, and as a Chinese medicine.[14] It has also been used as a red pigment in the Western world. A large amount of cinnabar has been found in ancient tombs because of its antiseptic properties.

The study of the highly enantioselective synthesis of organic compounds, utilizing cinnabar as the origin of chirality, is challenging. Herein, we report that the enantioselective addition of iPr$_2$Zn to pyrimidine-5-carbaldehyde **1** in the presence of cinnabar gave almost enantiopure 5-pyrimidyl alkanol **2** in conjunction with asymmetric autocatalysis (Figure 1c). The absolute configurations of organic compounds with high *ee* were efficiently controlled by the chirality of inorganic cinnabar. Furthermore, mechanistic insight into the asymmetric induction on the chiral (10–10) surface of α-HgS, gained through atomic force microscopy (AFM) results, is discussed.

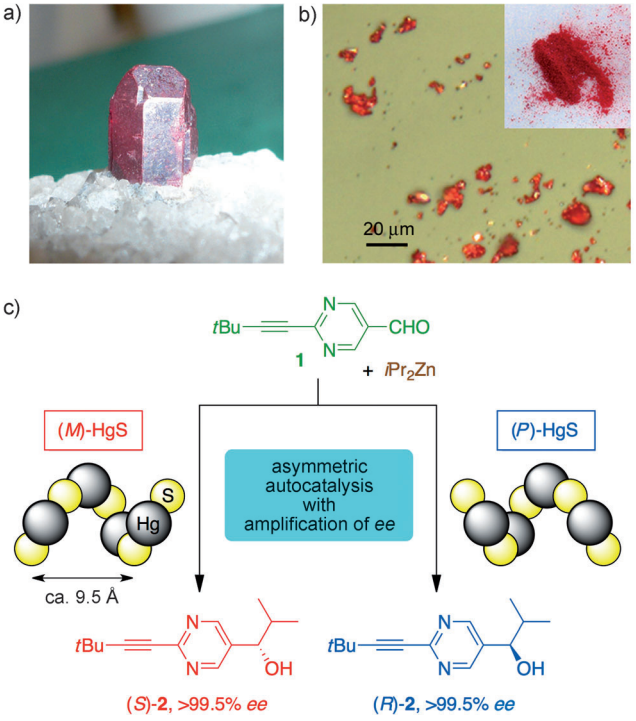

Figure 1. a) Cinnabar. b) Finely powdered cinnabar (particle size, 1–15 μm). c) Asymmetric autocatalysis triggered by (*P*)-HgS and (*M*)-HgS.

We performed an asymmetric autocatalysis initiated by cinnabar. Most of the crystals of known helicity[15] were ground into a fine powder (Figure 1b) and used as a heterogeneous chiral initiator in asymmetric autocatalysis (Table 1; see also Supporting Information, Table S2). When pyrimidine-5-carbaldehyde **1** was treated with iPr$_2$Zn in the presence of cinnabar **A**, which has right-handed *P* helicity, (*R*)-pyrimidyl alkanol **2** was obtained in 88% *ee* and 87% yield (Table 1, entry 1). In contrast, in the presence of the (*M*)-HgS

[*] Prof. Dr. H. Shindo, Y. Shirota, K. Niki
Department of Applied Chemistry, Chuo University
Kasuga, Bunkyo-ku, Tokyo 112-8551 (Japan)
E-mail: shindo@kc.chuo-u.ac.jp
Prof. Dr. T. Kawasaki,[+] Dr. K. Suzuki, Y. Araki, Dr. A. Matsumoto, Prof. Dr. K. Soai
Department of Applied Chemistry, Tokyo University of Science
Kagurazaka, Shinjuku-ku, Tokyo 162-8601 (Japan)
E-mail: soai@rs.kagu.tus.ac.jp
Prof. Dr. T. Kawasaki,[+] Prof. Dr. K. Soai
Research Center for Chirality, Research Institute for Science and Technology (RIST), Tokyo University of Science (Japan)
[+] Present address: Department of Materials Science and Engineering, University of Fukui, Bunkyo, Fukui, 910-8507 (Japan)

[**] This work was supported by a Grant-in-Aid for Scientific Research from Japan Society for the Promotion of Science (JSPS) and MEXT-Supported Program for the Strategic Research Foundation at Private Universities, 2012–2016.
Supporting information for this article is available on the WWW under http://dx.doi.org/10.1002/anie.201304284.

Table 1: Asymmetric autocatalysis triggered by cinnabar.

Entry[a]	Cinnabar		Pyrimidyl alkanol **2**		
	Specimen	Helicity	Yield [%]	*ee* [%]	Configuration
1	**A**	*P*	87	88	*R*
2	**C**	*M*	91	92	*S*
3	**E**	*P*	77	86	*R*
4	**F**	*M*	88	88	*S*
5	**G**	*P*	87	92	*R*
6	**H**	*M*	90	87	*S*
7	**I**	*P*	89	87	*R*
8[b]	**J**	*M*	94	>99.5	*S*
9[b]	**K**	*P*	94	>99.5	*R*

[a] Unless otherwise noted, the molar ratio of α-HgS/**1**/*i*Pr$_2$Zn was 0.09:0.53:1.18. Aldehyde **1** and *i*Pr$_2$Zn were added in three separate portions (see the Supporting Information). [b] An additional consecutive asymmetric autocatalysis was applied.[5b]

C, the opposite enantiomer of (*S*)-**2** was isolated in 91 % yield and 92 % *ee* (entry 2). In entry 3, another specimen of (*P*)-HgS **E** was reacted. The correlation between the *P* helicity and the *R* configuration of **2** was reproducible (entry 3). When cinnabars **F**–**K** were utilized as the chiral sources, (*M*)-HgS species **F**, **H**, and **J** induced the formation of (*S*)-alkanol **2** (entries 4, 6, and 8), whereas (*P*)-cinnabars **G**, **I**, and **K** acted as chiral triggers for production of (*R*)-**2** (entries 5, 7, and 9). It should be noted that nearly enantiopure (*S*)-**2** and (*R*)-**2** (>99.5 % *ee*) were obtained by applying consecutive asymmetric autocatalysis (entries 8 and 9).[5b] Stereochemical correlations between specimens **A**–**K** and alkanol **2** were completely reproducible (Table S2).

These results show that the chiral cinnabar controls the absolute configuration of the resulting alkanol **2**. Therefore, adsorption structures[16] of related compounds were studied using AFM to address the chiral effect on the surface of cinnabar. Because cinnabar shows perfect cleavage on prismatic {10–10} surfaces parallel to the *c* axis,[17] the sides of the helices are mostly exposed to the solution for asymmetric autocatalysis. Thus, the crystal was cleaved into thin plates along the (10–10) direction to be used in adsorption experiments.

The AFM image (Fourier-transform filtered) of a cleaved bare (10–10) surface of (*P*)-HgS is shown in Figure 2a. The rectangular unit cell corresponds to the 950 × 415 pm unit cell in the X-ray-structure-based surface model (Figure 2b). The S atoms at the highest level produce the AFM spot pattern, and the additional bright spots within the unit cells may correspond to the S atoms at the second-highest level. The image in Figure 2c was observed after the (10–10) surface of (*P*)-HgS was soaked in a solution of aldehyde **1**. The spacing of the surface unit cell indicates that one molecule **1** occupies two unit cells. The AFM image shown in Figure 2d was observed after the adsorption of (*R*)-**2** at (*P*)-HgS. The periodicity of the spot pattern in the direction of the *c* axis is nearly the same as the HgS unit cell. Because molecule **2**, which has bulky *tert*-butyl and isopropyl groups on both ends, is large (ca. 1200 pm) compared with the size of the HgS unit cell, not every unit cell accommodates a molecule **2**. However, the proximity of the bright spots, most probably from the bulky groups, along the a_2 axis suggests attraction between the

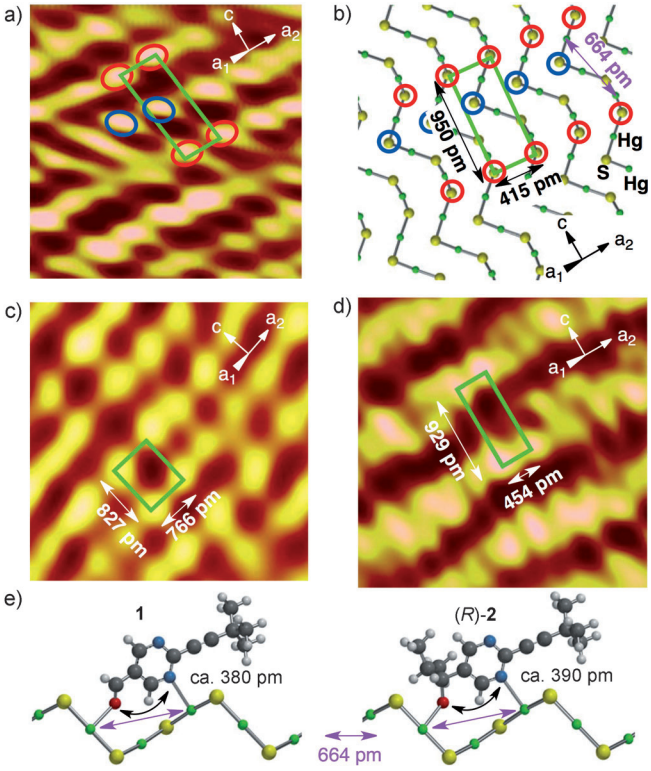

Figure 2. a) AFM images of the (10–10) surface of bare (*P*)-HgS (3.5 nm sq.). b) Model of the (10–10) surface of (*P*)-HgS. c) Aldehyde **1** adsorbed at the (*P*)-HgS (5.0 nm sq.). d) (*R*)-**2** adsorbed at (*P*)-HgS (3.4 nm sq.). e) Proposed adsorption geometries of **1** and (*R*)-**2** at (*P*)-HgS. S atoms of the highest level (red circles), S atoms of the second-highest level (blue circles), surface unit cell (green rectangles).

adsorbed molecules. It should be noted that similar AFM images were observed using (*S*)-**2** and (*M*)-HgS.

The well-resolved regular spot pattern in AFM images shown in Figure 2c,d indicates rigid bidentate adsorption,[18] which is possible using a N atom of the pyrimidine ring and an O atom of the formyl group for **1**, or the hydroxyl group for **2**, as anchor sites. The adsorption site with a Hg–Hg distance of 664 pm in Figure 2b is a good candidate for bidentate adsorption of both **1** and **2**. The proposed simple models of the adsorption geometries of **1** and (*R*)-**2** at (*P*)-HgS are shown in Figure 2e.

The AFM images in Figure 3a,b were observed after prolonged (>12 h) soaking of (*P*)- and (*M*)-HgS with (*R*)-**2** and (*S*)-**2**, respectively. Kite-shaped tetragonal islands with a width of ca. 200 nm and heights of 20–70 nm were formed. Because the tetragons have the same shape and orientation and were soluble in the pure solvent, microcrystal formation was assumed. However, microcrystals did not appear in experiments with the diastereomeric pairs (*R*)-**2**/(*M*)-HgS and (*S*)-**2**/(*P*)-HgS (Figure S3). Thus, the molecular chirality of alkanol **2** was recognized on the chiral surface of HgS in the formation of three-dimensional structures. Figure 3c shows the X-ray single-crystal structure of (*S*)-**2** (orthorhombic $P2_12_12_1$, $a' = 599.99$ pm, $b' = 829.46$ pm, $c' = 2726.96$ pm, $Z = 4$).[19] The molecules are combined in the a'-c' plane, mainly by hydrogen bonds. Hydrophobic interactions connect the molecules along the c' direction.

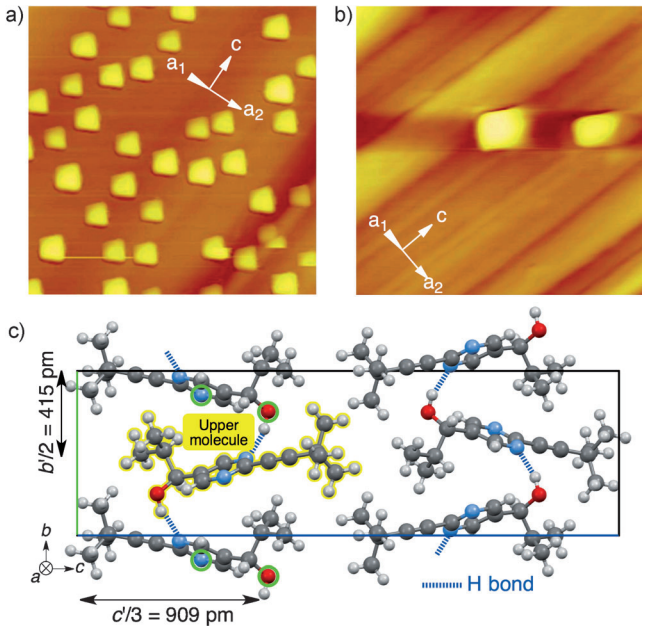

Figure 3. AFM images of microcrystals of a) (*R*)-**2** at (*P*)-HgS (2.0 μm sq.) and b) (*S*)-**2** at (*M*)-HgS (1.5 μm sq.). c) X-ray single-crystal structure of (*S*)-**2**. Atoms proposed as anchor sites are indicated by green circles.

A possible mechanism for the selective formation of a microcrystal is as follows: when molecules of **2** with the chosen configuration adsorb at the surface with a regular spacing of two unit-cell widths, as can be seen in the case of aldehyde **1** using the atoms indicated by green circles (Figure 3c) as anchor sites, new binding sites are created between the two molecules only for the alkanols **2** with the same configuration. Then, the adsorption of the upper molecules gives a chiral three-dimensional structure, and further adsorption onto the upper layers induces microcrystal formation. Because inappropriate combinations would lead to two-dimensional adsorption in a different direction, formation of a chiral three-dimensional structure occurs only when the combinations of chirality between HgS and alkanol **2** are appropriate.

Although we assumed enantioselective adsorption of the initially formed near-racemic asymmetric autocatalyst for chiral selection, (*P*)-HgS induced the formation of (*R*)-**2** and the same *R* isomer also formed the microcrystal on (*P*)-HgS and vice versa. As the reactive species is a diisopropylzinc alkoxide of alkanol **2**, it is difficult to consider that the microcrystal formation of alkanol **2** directly affects the enantioselection step. Therefore, it is conceivable that a chiral effect, such as the formation of a three-dimensional structure of a diisopropylzinc alkoxide of alkanol **2**, would occur in a similar manner to induce the imbalance of enantiomers, which can be amplified by asymmetric autocatalysis. Moreover, enantiofacially selective adsorption (activation) of prochiral aldehyde **1** on the chiral surface of cinnabar is also good candidate for the mechanism of asymmetric induction.

In conclusion, highly enantioselective addition of $i\mathrm{Pr}_2\mathrm{Zn}$ to pyrimidine-5-carbaldehyde **1** was achieved to afford a highly enantioenriched organic compound by utilizing naturally occurring enantiomorphous cinnabar. Moreover, adsorption structures of aldehyde **1** and alkanol **2** were observed using AFM in contact mode. For the first time, a chiral effect in the formation of microcrystals of **2** was found on the surface of chiral cinnabar.

Received: May 18, 2013
Published online: July 23, 2013

Keywords: asymmetric amplification · atomic force microscopy · autocatalysis · cinnabar · homochirality

[1] a) M. Bolli, R. Micura, A. Eschenmoser, *Chem. Biol.* **1997**, *4*, 309–320; b) I. Weissbuch, M. Lahav, *Chem. Rev.* **2011**, *111*, 3236–3267; c) B. Kahr, R. W. Gurney, *Chem. Rev.* **2001**, *101*, 893–951; d) K. Mislow, *Collect. Czech. Chem. Commun.* **2003**, *68*, 849–864; e) B. L. Feringa, R. A. van Delden, *Angew. Chem.* **1999**, *111*, 3624–3645; *Angew. Chem. Int. Ed.* **1999**, *38*, 3418–3438; f) M. M. Green, J.-W. Park, T. Sato, A. Teramoto, S. Lifson, R. L. B. Selinger, J. V. Selinger, *Angew. Chem.* **1999**, *111*, 3329–3345; *Angew. Chem. Int. Ed.* **1999**, *38*, 3139–3154; g) C. Girard, H. B. Kagan, *Angew. Chem.* **1998**, *110*, 3088–3127; *Angew. Chem. Int. Ed.* **1998**, *37*, 2922–2959; h) D. K. Kondepudi, K. Asakura, *Acc. Chem. Res.* **2001**, *34*, 946–954; i) J. M. Ribo, J. Crusats, F. Sagues, J. Claret, R. Rubires, *Science* **2001**, *292*, 2063–2066; j) A. Guijarro, M. Yus, *The Origin of Chirality in the Molecules of Life*, Royal Society Chemistry, Cambridge, **2009**; k) Y. Saito, H. Hyuga, *Rev. Mod. Phys.* **2013**, *85*, 603–621.

[2] a) *Chirality at the nanoscale, nanoparticles, surfaces, materials and more* (Ed.: D. B. Amabilino), Wiley-VCH, Weinheim, **2009**; b) K.-H. Ernst, *Phys. Status Solidi B* **2012**, *249*, 2057–2088; c) R. Raval, *Chem. Soc. Rev.* **2009**, *38*, 707–721; d) L. P. Garciaa, D. B. Amabilino, *Chem. Soc. Rev.* **2007**, *36*, 941–967.

[3] a) R. M. Hazen in *Progress in biological chirality* (Eds.: G. Palyi, C. Zucchi), Elsevier, Oxford, **2004**, Chap. 9, pp. 137–151; b) R. M. Hazen, D. S. Sholl, *Nat. Mater.* **2003**, *2*, 367–374; c) L. Vega, J. Breton, G. Girardet, L. Galatry, *J. Chem. Phys.* **1986**, *84*, 5171–5180.

[4] a) B. Kahr, B. Chittenden, A. Rohl, *Chirality* **2006**, *18*, 127–133; b) W. A. Bonner, P. R. Kavasmaneck, F. S. Martin, J. J. Flores, *Science* **1974**, *186*, 143–144; c) R. M. Hazen, T. R. Filley, G. A. Goodfriend, *Proc. Natl. Acad. Sci. USA* **2001**, *98*, 5487–5490.

[5] a) K. Soai, T. Shibata, H. Morioka, K. Choji, *Nature* **1995**, *378*, 767–768; b) I. Sato, H. Urabe, S. Ishiguro, T. Shibata, K. Soai, *Angew. Chem.* **2003**, *115*, 329–331; *Angew. Chem. Int. Ed.* **2003**, *42*, 315–317; c) T. Shibata, T. Hayase, J. Yamamoto, K. Soai, *Tetrahedron: Asymmetry* **1997**, *8*, 1717–1719.

[6] a) T. Kawasaki, I. Sato, H. Mineki, A. Matsumoto, K. Soai, *J. Synth. Org. Chem. Jpn.* **2013**, *71*, 109–123; b) T. Kawasaki, A. Matsumoto, K. Soai, *Chim. Oggi* **2012**, *30*, 10–13; c) T. Kawasaki, K. Soai, *Bull. Chem. Soc. Jpn.* **2011**, *84*, 879–892; d) K. Soai, T. Kawasaki, T. Shibata, *Catalytic asymmetric synthesis, 3rd ed.* (Ed.: I. Ojima), Wiley, Hoboken, New Jersey, **2010**, pp. 891–930; e) K. Soai, T. Kawasaki, *Chirality* **2006**, *18*, 469–478; f) K. Soai, T. Kawasaki, *Top. Curr. Chem.* **2008**, *284*, 1–33.

[7] a) J.-K. Micheau, C. Coudret, T. Buhse, *The Soai Reaction and Related Topics* (Eds.: G. Palyi, C. Zucchi, L. Caglioti), Accad. Nazl. Sci. Lett. Arti Modena, Modena, **2012**, Chap. 7, pp. 169–196; b) T. Gehring, M. Busch, M. Schlageter, D. Weingand, *Chirality* **2010**, *22*, E173–E182; c) B. Barabás, J. Toth, G. Pályi, *J. Math. Chem.* **2010**, *48*, 457–489; d) G. Lente, *Symmetry* **2010**, *2*, 767–798; e) J. M. Brown, I. Gridnev, J. Klankermayer, *Top.*

Curr. Chem. **2008**, *284*, 35 – 65; f) L. Caglioti, G. Palyi, *Chim. Oggi* **2008**, *26*, 41 – 42.

[8] For mechanistic analyses, see: a) I. Sato, D. Omiya, H. Igarashi, K. Kato, Y. Ogi, K. Tsukiyama, K. Soai, *Tetrahedron: Asymmetry* **2003**, *14*, 975 – 979; b) M. Quaranta, T. Gehring, B. Odell, J. M. Brown, D. G. Blackmond, *J. Am. Chem. Soc.* **2010**, *132*, 15104 – 15107; c) G. Ercolani, L. Schiaffino, *J. Org. Chem.* **2011**, *76*, 2619 – 2626; d) J.-C. Micheau, C. Coudret, J.-M. Cruz, T. Buhse, *Phys. Chem. Chem. Phys.* **2012**, *14*, 13239 – 13248; e) T. Gehring, M. Quaranta, B. Odell, D. G. Blackmond, J. M. Brown, *Angew. Chem.* **2012**, *124*, 9677 – 9680; *Angew. Chem. Int. Ed.* **2012**, *51*, 9539 – 9542; f) I. D. Gridnev, A. K. Vorobiev, *ACS Catal.* **2012**, *2*, 2137 – 2149.

[9] a) K. Soai, S. Osanai, K. Kadowaki, S. Yonekubo, T. Shibata, I. Sato, *J. Am. Chem. Soc.* **1999**, *121*, 11235 – 11236; b) I. Sato, K. Kadowaki, K. Soai, *Angew. Chem.* **2000**, *112*, 1570 – 1572; *Angew. Chem. Int. Ed.* **2000**, *39*, 1510 – 1512.

[10] a) T. Kawasaki, Y. Matsumura, T. Tsutsumi, K. Suzuki, M. Ito, K. Soai, *Science* **2009**, *324*, 492 – 495; b) T. Kawasaki, M. Sato, S. Ishiguro, T. Saito, Y. Morishita, I. Sato, H. Nishino, Y. Inoue, K. Soai, *J. Am. Chem. Soc.* **2005**, *127*, 3274 – 3275; c) K. Soai, I. Sato, T. Shibata, S. Komiya, M. Hayashi, Y. Matsueda, H. Imamura, T. Hayase, H. Morioka, H. Tabira, J. Yamamoto, Y. Kowata, *Tetrahedron: Asymmetry* **2003**, *14*, 185 – 188.

[11] K. L. Aurivillius, *Acta Chem. Scand.* **1950**, *4*, 1413 – 1436.

[12] B. Pal, S. Ikeda, B. Ohtani, *Inorg. Chem.* **2003**, *42*, 1518 – 1524.

[13] A. Ben-Moshe, A. O. Govorov, G. Markovich, *Angew. Chem.* **2013**, *125*, 1313 – 1317; *Angew. Chem. Int. Ed.* **2013**, *52*, 1275 – 1279.

[14] H. G. M. Edwards, *Asian J. Phys.* **1998**, *7*, 383 – 389.

[15] Seven (*P*)-HgS and seven (*M*)-HgS species were found among specimens **A**–**N** by X-ray single crystal analysis (Supporting Information, Table S1).

[16] D. J. Carter, A. L. Rohl, A. Shtukenberg, S. Bian, C. Hu, L. Baylon, B. Kahr, H. Mineki, K. Abe, T. Kawasaki, K. Soai, *Cryst. Growth Des.* **2012**, *12*, 2138 – 2145.

[17] E. S. Dana, in The System of Mineralogy -Descriptive Mineralogy, *6th ed.*, Wiley, New York, **1900**, pp. 66 – 67.

[18] A well-resolved AFM image of HgS treated with pyrimidine indicates bidentate adsorption (Supporting Information, Figure S2).

[19] CCDC 938819 ((*S*)-**2**) contains the supplementary crystallographic data for this paper. These data can be obtained free of charge from The Cambridge Crystallographic Data Centre via www.ccdc.cam.ac.uk/data_request/cif.

